"Nuclear effects and reconstruction of neutrino CCQE scattering cross sections on nuclei"

Anatoli Butkevich (INR, Moscow)

Talk at "Neutrino physics at accelerators" Workshop, Dubna, January 27, 2009

- Motivations.
- Formalism of the charged-current (CC) quasi-elastic (QE) scattering.
- Analysis of the CCQE interaction and neutrino energy reconstruction.
- Results.
- Summary.

For more details of the present approach see:
A.Butkevich, S.Mikheyev,Phys.Rev.C72:025501,2005;
A.Butkevich, S.Kulagin,Phys.Rev.C76:045502,2007;
A.Butkevich,Phys.Rev.C78:015501,2008

Motivations

- To study the neutrino oscillation effects on the terrestrial distance scale the intense neutrino beam cover the energy range from a few 100 MeV to a few GeV.
- In this energy range the neutrino nuclear scattering is dominated by (QE) scattering from bound nucleons and resonance production. An important source of systematic uncertainties is due to nuclear effects in neutrino interactions.
- Most event generators to model the scattering from nuclei are based on the Relativistic Fermi Gas Model (RFGM). High-precision QE electron and neutrinos scattering data are show that the accuracy of the RFGM prediction becomes poor at low Q^2 where the nuclear effects are largest.
- Within the Relativistic Distorted-Wave Impulse Approximation (RDWIA) we study neutrino-nuclear scattering and analyses:
  - (⋆) CCQE inclusive cross section $d\sigma/dQ^2$ and nuclear effects
  - (⋆) nuclear-model dependence of the two-track CCQE events selection efficiency
- Systematic uncertainties of the reconstructed neutrino energy
  - (⋆) kinematic and calorimetric methods
  - (⋆) kinematic method: nucleon Fermi motion effect and nuclear-model dependence of the reconstructed neutrino energy

Formalism of the quasi-elastic scattering

We consider lepton CCQE exclusive

$$l(k_i) + A(p_A) \longrightarrow l'(k_f) + N(p_x) + B(p_B),$$

and inclusive

$$l(k_i) + A(p_A) \longrightarrow l'(k_f) + X$$

scattering off nuclei, where

- ⋆ l is incident (anti)neutrino, l' is scattered lepton (e/μ), $k_i = (\varepsilon_i, \boldsymbol{k}_i)$ and $k_f = (\varepsilon_f, \boldsymbol{k}_f)$ are initial and final lepton momenta
- ⋆ $p_A = (\varepsilon_A, \boldsymbol{p}_A)$, and $p_B = (\varepsilon_B, \boldsymbol{p}_B)$ are the initial and final target momenta, $p_x = (\varepsilon_x, \boldsymbol{p}_x)$ is ejectile nucleon momentum
- ⋆ $q = (\omega, \boldsymbol{q})$ is momentum transfer carried by the virtual W-boson, and $Q^2 = -q^2 = \boldsymbol{q}^2 - \omega^2$ is W-boson virtuality
- ⋆ m, m_A and m_B are masses of nucleon, target and recoil nucleus, respectively. The missing energy and momentum are defined by $\boldsymbol{p}_m = \boldsymbol{p}_x - \boldsymbol{q}, \quad \varepsilon_m = m + m_B - m_A$

A. QE lepton-nucleus cross section

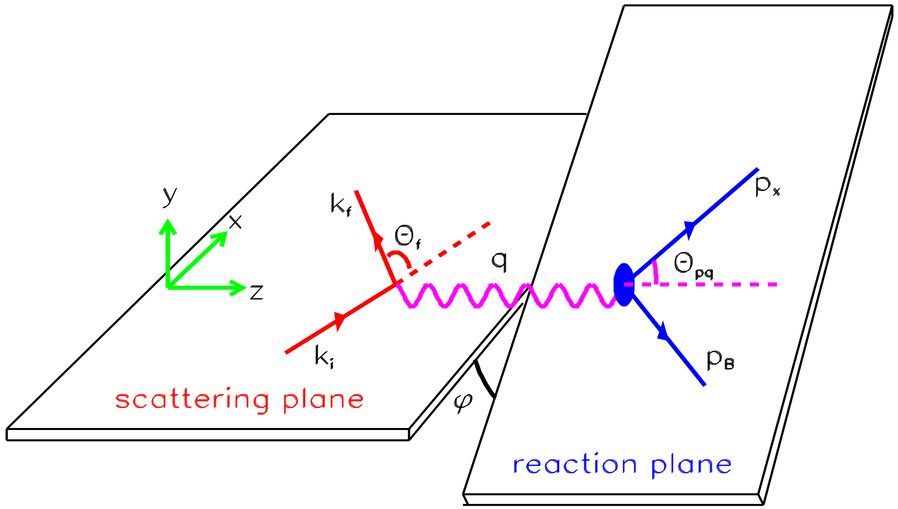

Kinematic definitions for A$(l, l'N)$B reactions.

In the lab frame the differential cross section for exclusive (anti)neutrino CC scattering can be written as

$$\frac{d^5\sigma}{d\varepsilon_f d\Omega_f d\Omega_x} = R\frac{|\boldsymbol{p}_x|\varepsilon_x}{(2\pi)^5}\frac{|\boldsymbol{k}_f|}{\varepsilon_i}\frac{G^2\cos^2\theta_c}{2}L_{\mu\nu}W^{\mu\nu},$$

where Ω_f is the solid angle for the lepton momentum, Ω_x is the solid angle for the ejectile nucleon momentum, $G \simeq 1.16639 \times 10^{-11}$ MeV^{-2} is the Fermi constant, θ_C is the Cabbibo angle ($\cos\theta_C \approx 0.9749$). The recoil factor R is given by

$$R = \left|1 - \frac{\varepsilon_x}{\varepsilon_B}\frac{\boldsymbol{p}_x \cdot \boldsymbol{p}_B}{\boldsymbol{p}_x \cdot \boldsymbol{p}_x}\right|^{-1},$$

and ε_x is solution to equation $\varepsilon_x + \varepsilon_B - m_A - \omega = 0$, where $\varepsilon_B = \sqrt{m_B^2 + \boldsymbol{p}_B^2}$, $\boldsymbol{p}_B = \boldsymbol{q} - \boldsymbol{p}_x = -\boldsymbol{p}_m$, $\boldsymbol{p}_x = \sqrt{\varepsilon_x^2 - m^2}$, and m_A, m_B, and m are masses of the target, recoil nucleus, and nucleon respectively.

A useful quantity to compare nuclear calculations for electron and neutrino scattering is reduced cross section

$$\sigma_{red} = \frac{d^5\sigma}{d\varepsilon_f d\Omega_f d\Omega_x}/K\sigma_{lN},$$

where $K = Rp_x\varepsilon_x/(2\pi)^5$ are phase-space factors for neutrino scattering and σ_{lN} is elementary cross section for the lepton scattering from moving free nucleon.

The lepton tensor can be written as the sum of symmetric $L_S^{\mu\nu}$ and antisymmetric $L_A^{\mu\nu}$ tensors

$$
\begin{aligned}
L^{\mu\nu} &= L_S^{\mu\nu} + L_A^{\mu\nu} \\
L_S^{\mu\nu} &= 2\left(k_i^{\mu} k_f^{\nu} + k_i^{\nu} k_f^{\mu} - g^{\mu\nu} k_i k_f\right) \\
L_A^{\mu\nu} &= h 2i\epsilon^{\mu\nu\alpha\beta}(k_i)_{\alpha}(k_f)_{\beta},
\end{aligned}
$$

where h is $+1$ for positive lepton helicity and -1 for negative lepton helicity, $\epsilon^{\mu\nu\alpha\beta}$ is the antisymmetric tensor

The weak CC hadronic tensors $W_{\mu\nu}$ is given by bilinear products of the transition matrix elements of the nuclear CC operator J_{μ} between the initial nucleus state $|A\rangle$ and the final state $|B_f\rangle$ as

$$
W_{\mu\nu} = \sum_f \langle B_f, p_x | J_{\mu} | A\rangle \langle A | J_{\nu} | B_f, p_x\rangle
$$

where the sum is taken over undetected states.

In the inclusive reactions only the outgoing lepton is detected and the differential cross sections can be written as

$$\frac{d^3\sigma}{d\varepsilon_f d\Omega_f} = \frac{1}{(2\pi)^2}\frac{|\boldsymbol{k}_f|}{\varepsilon_i}\frac{G^2\cos^2\theta_c}{2}L_{\mu\nu}\mathcal{W}^{\mu\nu},$$

where $\mathcal{W}^{\mu\nu}$ is inclusive hadronic tensor.

- We describe the lepton-nucleon scattering in the Impulse Approximation (IA), in which only one nucleon of the target is involved in reaction and the nuclear current is written as the sum of single-nucleon currents. Then, the nuclear matrix element takes the form

$$\langle p, B|J^\mu|A\rangle = \int d^3r \ \exp(i\boldsymbol{t}\cdot\boldsymbol{r})\overline{\Psi}^{(-)}(\boldsymbol{p},\boldsymbol{r})\Gamma^\mu\Phi(\boldsymbol{r}),$$

  where Γ^μ is the vertex function, $\boldsymbol{t} = \varepsilon_B\boldsymbol{q}/W$ is the recoil-corrected momentum transfer, $W = \sqrt{(m_A+\omega)^2 - \boldsymbol{q}^2}$ is the invariant mass, Φ and $\Psi^{(-)}$ are relativistic bound-state and outgoing wave functions.

- The single-nucleon charged current has $V-A$ structure $J^\mu = J^\mu_V + J^\mu_A$. For a free nucleon vertex function $\Gamma^\mu = \Gamma^\mu_V + \Gamma^\mu_A$ we use CC2 vector current vertex function

$$\Gamma^\mu_V = F_V(Q^2)\gamma^\mu + i\sigma^{\mu\nu}\frac{q_\nu}{2m}F_M(Q^2)$$

and the axial current vertex function

$$\Gamma_A^\mu = F_A(Q^2)\gamma^\mu\gamma_5 + F_P(Q^2)q^\mu\gamma_5.$$

Weak vector form factors F_V and F_M are related to corresponding electromagnetic ones for proton $F_{i,p}^{(el)}$ and neutron $F_{i,n}^{(el)}$ by the hypothesis of conserved vector current (CVC)

$$F_i = F_{i,p}^{(el)} - F_{i,n}^{(el)},$$

where $F_V^{(el)}$ and $F_M^{(el)}$ are the Dirac and Pauli nucleon form factors. We use the MMD approximation [P.Mergell et al (1996)] of the nucleon form factors.

- Because the bound nucleons are off shell, we use de Forest prescription for off-shell [T. de Forest (1983)] extrapolation of Γ^μ and Coulomb gauge is applied for the vector current J_V.
- The axial F_A and psevdoscalar F_P form factors in the dipole approximation are parameterized as

$$F_A(Q^2) = \frac{F_A(0)}{(1+Q^2/M_A^2)^2}, \quad F_P(Q^2) = \frac{2mF_A(Q^2)}{m_\pi^2+Q^2},$$

where $F_A(0) = 1.267$, m_π is the pion mass, and $M_A \simeq 1.032$ GeV is the axial mass.

Independ Particle Shell Model

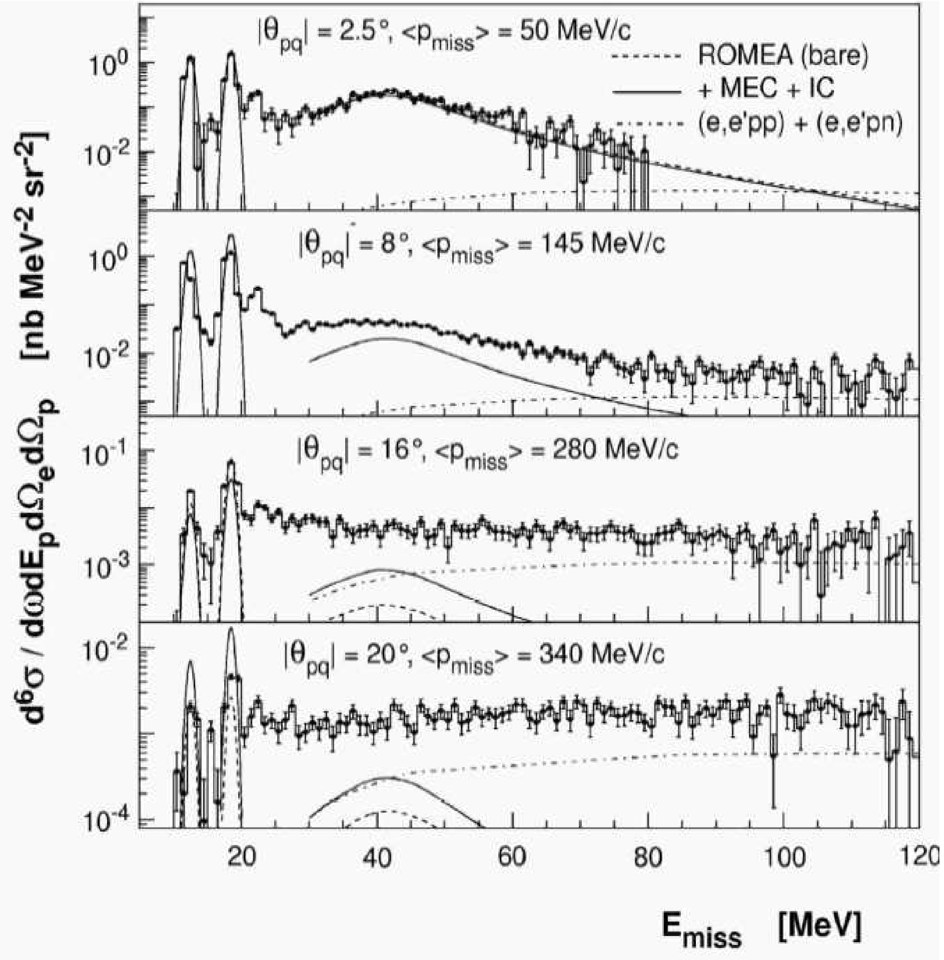

Shell occupancy for Oxygen:

S($P_{1/2}$)=0.7

S($P_{3/2}$)=0.66

S($S_{1/2}$)=1

Average occupancy of nuclear shells $\overline{S}$=0.75
[supported by JLab measurement K. G. Fissum et al. (2005)]

Missing Energy
Neutron: $\varepsilon(1p_{1/2})$=15.7 MeV, $\varepsilon_m(1p_{3/2})$=21.2 MeV, $\varepsilon_m(1s_{1/2})$=42.9 MeV
Proton: $\varepsilon_m(1p_{1/2})$=12.1 MeV, $\varepsilon_m(1p_{3/2})$=18.4 MeV, $\varepsilon_m(1s_{1/2})$=40.1 MeV

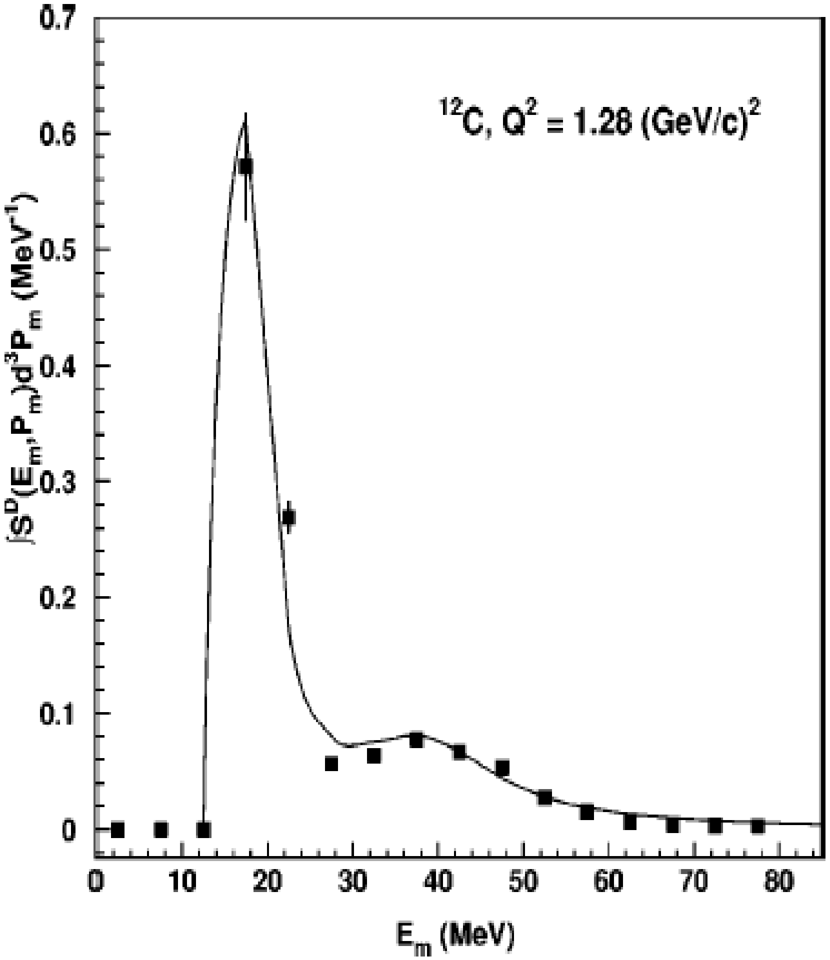

Shell occupancy for Carbon:

S($P_{3/2}$)=0.84

S($S_{1/2}$)=1

Average occupancy of nuclear shells $\overline{S}$=0.89
[supported by JLab measurement D. Dutta et al. (2003)] and [J.J.Kelly (2004)]

Missing Energy
Neutron: $\varepsilon_m(1p_{3/2})$=17.9 MeV, $\varepsilon_m(1s_{1/2})$=39.8 MeV
Proton: $\varepsilon_m(1p_{3/2})$=16 MeV, $\varepsilon_m(1s_{1/2})$=37.9 MeV

Missing strength can be attributed to the short-range NN-correlations in ground state.

Relativistic Distorted Wave Impulse Approximation

Bound state wave functions

In independ particle shell model the relativistic bound-state functions Φ are obtained within the Hartree–Bogolioubov approximation in the $\sigma - \omega$ model [B.Serot et al. 1986] The bound-state spinor takes the form

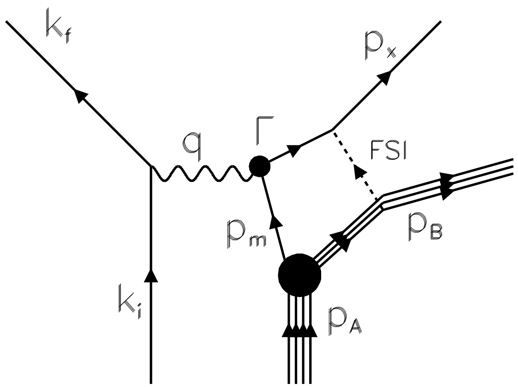

$$\Phi_{\kappa m}(\mathbf{r}) = \begin{pmatrix} F_\kappa(r)\mathcal{Y}_{\kappa m}(\hat{r}) \\ iG_{-\kappa}(r)\mathcal{Y}_{-\kappa m}(\hat{r}) \end{pmatrix},$$

where

$$\mathcal{Y}_{\kappa m}(\hat{r}) = \sum_{\nu, m_s} \left\langle \begin{array}{cc} \ell & \frac{1}{2} \\ \nu & m_s \end{array} \middle| \begin{array}{c} j \\ m \end{array} \right\rangle Y_{\ell\nu}(\hat{r})\chi_{m_s}$$

is the spin spherical harmonic and where the orbital and total angular momenta are respectively given by

$$\ell = S_\kappa(\kappa + \frac{1}{2}) - \frac{1}{2}$$

$$j = S_\kappa \kappa - \frac{1}{2}, \qquad S_\kappa = sign(\kappa).$$

The missing momentum distribution is then

$$P(p_m) = \frac{S_\alpha}{2\pi^2}\left(|\tilde{F}_\kappa(p_m)|^2 + |\tilde{G}_\kappa(p_m)|^2\right),$$

where

$$\begin{aligned}\tilde{F}_\kappa(p) &= \int dr\ r^2 j_\ell(p_m r) F_\kappa(r) \\ \tilde{G}_{-\kappa}(p) &= \int dr\ r^2 j_{\ell'}(p_m r) G_{-\kappa}(r),\end{aligned}$$

and $j_\ell(x)$ is the Bessel function of order ℓ and $\ell' = 2j - \ell$.

Outgoing state wave functions

In the RDWIA the ejectile wave function Ψ is obtained following the direct Pauli reduction method. It is well known that Dirac spinor

$$\Psi = \begin{pmatrix}\Psi_+ \\ \Psi_-\end{pmatrix}$$

can be written in terms of its positive energy component Ψ_+ as

$$\Psi = \begin{pmatrix}\Psi_+ \\ \frac{\boldsymbol{\sigma}\cdot\boldsymbol{p}}{E+M+S-V}\Psi_+,\end{pmatrix}$$

where $S = S(r)$ and $V = V(r)$ are the scalar and vector potentials for the nucleon with energy E. The upper component Ψ_+ can be related to a Schrödinger-like wave function ξ by the Darwin factor $D(r)$, i.e.

$$\Psi_+ = \sqrt{D(r)}\,\xi,$$

$$D(r) = \frac{E + M + S(r) - V(r)}{E + M}.$$

The two-component wave function ξ is solution of a Schrödinger equation containing equivalent central and spin-orbit potentials, which are functions of the scalar and vector potentials S and V, and are energy dependent.

We use the LEA program [J.J. Kelly (1995)] for numerical calculation of the distorted wave functions with EDAD1 SV relativistic optical potential [E. Cooper (1993)].

The RDWIA was pioneered by [Picklesimer, Van Orden, and Wallace (1985,1987,1989)] and developed in more detail by several groups [J.P.McDermott et al. (1991), Y.Jin et al. (1992), J.Udias et al. (1993), M.Hedayati-Poor et al. (1995) J.J.Kelly (1999), A.Meucci et al (2001)]

Plane-Wave Impulse Approximation (PWIA)

In the PWIA the final state interaction between the outgoing nucleon and the residual nucleus is neglected. In nonrelativistic PWIA the knockout cross section has a factorized form

$$\frac{d^5\sigma}{d\varepsilon_f d\Omega_f d\Omega_x} = K\sigma_{ex}P(E,\boldsymbol{p})$$

where

$$K = R\frac{p_x\varepsilon_x}{(2\pi)^5}$$

are the phase-space factors, R is recoil factor, σ_{ex} is the half-off-shell cross section for scattering of a lepton by moving nucleon.

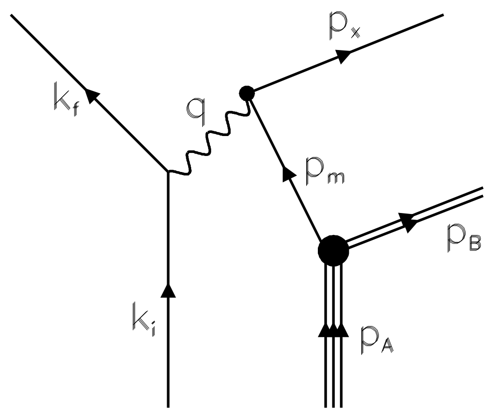

The nuclear spectral function P represents the probability of removing a nucleon with momentum $\boldsymbol{p}$ and energy E from the nuclear target A and leaving the residual nucleus B in the state with energy, $E = m + m_B - m_A$, where m_B and m_A are the nuclear masses in the corresponding states.

Fermi gas model

In the RFGM the nucleons are described as a system of quasi-free nucleons. This model takes into account the Fermi motion of bound nucleon, Pauli blocking factor and relativistic kinematics. The Fermi gas model provides a simplest form of the spectral function which is given by

$$P_{FG}(E,|\boldsymbol{p}|) = \frac{3}{4\pi p_F^3}\Theta(p_F - |\boldsymbol{p}|)\Theta(|\boldsymbol{p}+\boldsymbol{q}| - p_F) \times \delta[(\boldsymbol{p}^2 + m^2)^{1/2} - \varepsilon - E],$$

where p_F is the Fermi momentum and ε is effective binding energy, introduced to account of nuclear binding. For oxygen we use p_F=250 MeV/c, ε=27 MeV and for carbon p_F=221 MeV/c, ε=25 MeV.

The RFGM does not account nuclear shell structure, FSI effect, and the presence of NN-correlations.

NN-correlations in nuclear ground state

- According to JLab data [K. Fissum et al (2004), D.Dutta et al (2003), and J.J.Kelly (2004)] the occupancy of the IPSM orbitals of ^{16}O is approximately 75% on average and 89% for ^{12}C. We assume that the missing strength can be attributed to the short-range NN-correlations in the ground state.

- We consider a phenomenological model in PWIA, which incorporates high-energy and high-momentum component P_{HM} due to NN-correlations [C.Ciofi degli Atti et al (1996), S.Kulagin et al (2006)].

- In our calculations the spectral function P_{HM} incorporates 25% (11%) of the total normalization of the spectral function for ^{16}O (^{12}C).

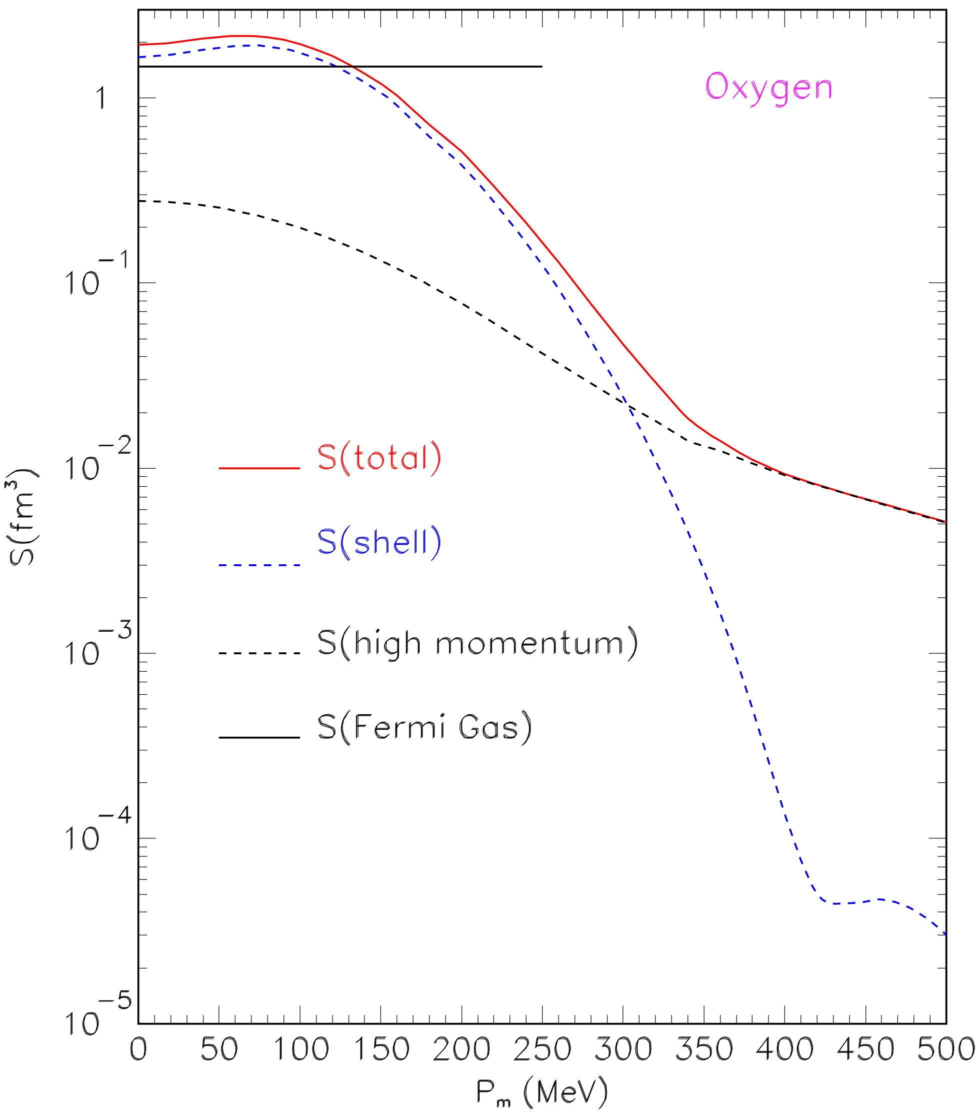

Momentum distribution for the NLSH models and hight-momentum component of the NN-corelation. The occupancy of the orbitals of ^{16}O is 75% on average and the spectral function P_{HM} incorporates 25% of the total normalization of the spectral function.

Inclusive and total cross sections

- In order to calculate inclusive and total cross sections, we use the approach, in which only the real part of the optical potential EDAD1 is included because a complex optical potential produces adsorbtion of flux. Then the contribution of the $1p$- and $1s$-states to the inclusive cross section can be obtained as follows:

$$\left(\frac{d^3\sigma}{d\varepsilon_f d\Omega_f}\right)_{RDWIA} = \int_0^{2\pi} d\phi \int_{p_{min}}^{p_{max}} dp_m \frac{p_m}{p_x|\boldsymbol{q}|} R_c \times \left(\frac{d^5\sigma}{d\varepsilon_f d\Omega_f d\Omega_x}\right)_{RDWIA},$$

  The effect of the FSI on the inclusive cross section can be evaluated using the ratio

$$\Lambda(\varepsilon_f, \Omega_f) = \left(\frac{d^3\sigma}{d\varepsilon_f d\Omega_f}\right)_{RDWIA} \Bigg/ \left(\frac{d^3\sigma}{d\varepsilon_f d\Omega_f}\right)_{PWIA},$$

  where $\left(d^3\sigma / d\varepsilon_f d\Omega_f\right)_{PWIA}$ is the result obtained in the PWIA.

- The FSI effect for the high-momentum component is estimated by scaling the PWIA result $(d^3\sigma/d\varepsilon_f d\Omega_f)_{HM}$ with $\Lambda(\varepsilon_f, \Omega_f)$ function. Then the total inclusive cross section can be written as

$$\frac{d^3\sigma}{d\varepsilon_f d\Omega_f} = \left(\frac{d^3\sigma}{d\varepsilon_f d\Omega_f}\right)_{RDWIA} + \Lambda(\varepsilon_f, \Omega_f)\left(\frac{d^3\sigma}{d\varepsilon_f d\Omega_f}\right)_{HM}.$$

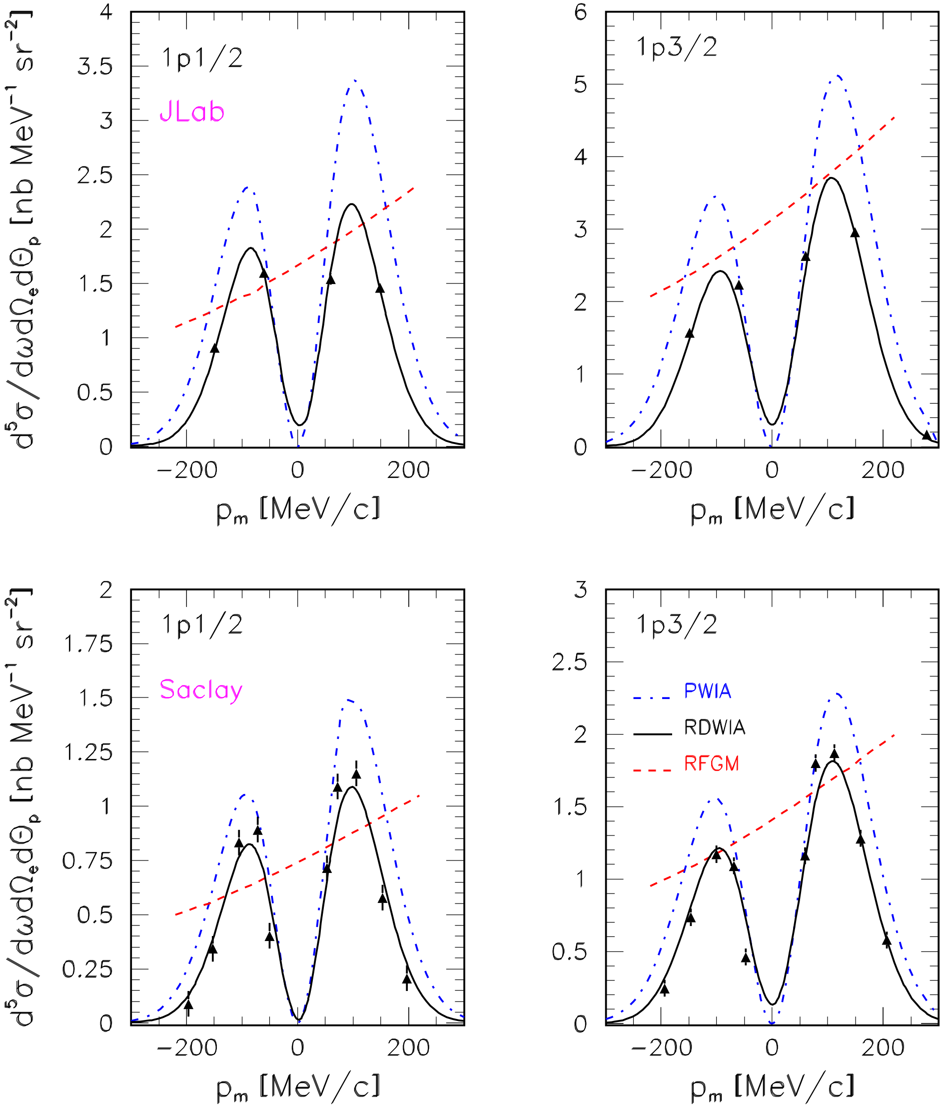

Measured differential exclusive cross-section data for the removal of protons from 1p-shell of ^{16}O as a function of missing momentum . The upper panels show JLab data for electron beam energy E_{beam}=2.442 GeV, proton kinetic energy T_p=427 MeV, and Q^2=0.8 GeV^2. The lower panels show Saclay data for E_{beam}=580 MeV, T_p=160 MeV, and Q^2=0.3 GeV^2. The solid line is the RDWIA calculation while the dashed-dotted and dashed lines are respectively the PWIA and RFGM calculations. Negative values of p_m correspond to $\phi = \pi$ and positive ones to $\phi = 0$.

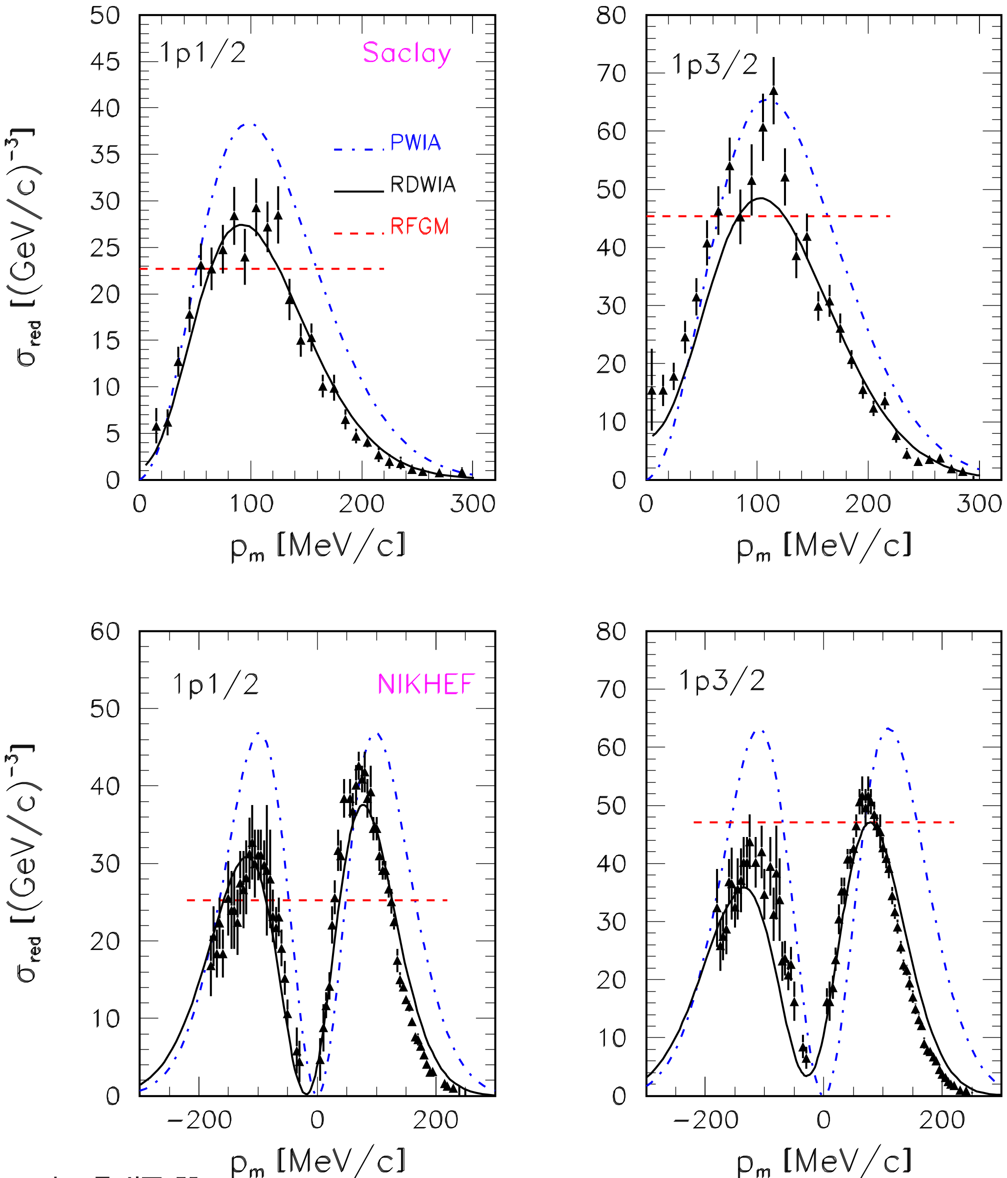

Measured reduced exclusive cross-section data for the removal of protons from 1p-shell of ^{16}O as a function of missing momentum. The upper panels show Saclay data for electron beam energy E_{beam}=500 MeV, proton kinetic energy T_p=100 MeV, and Q^2=0.3 GeV^2. The lower panels show NIKHEF data for E_{beam}=521 MeV, T_p=96 MeV, Q^2 is varied. The solid line is the RDWIA calculation while the dashed-dotted and dashed lines are respectively the PWIA and RFGM calculations.

The RFGM predictions are completely off of the exclusive data.

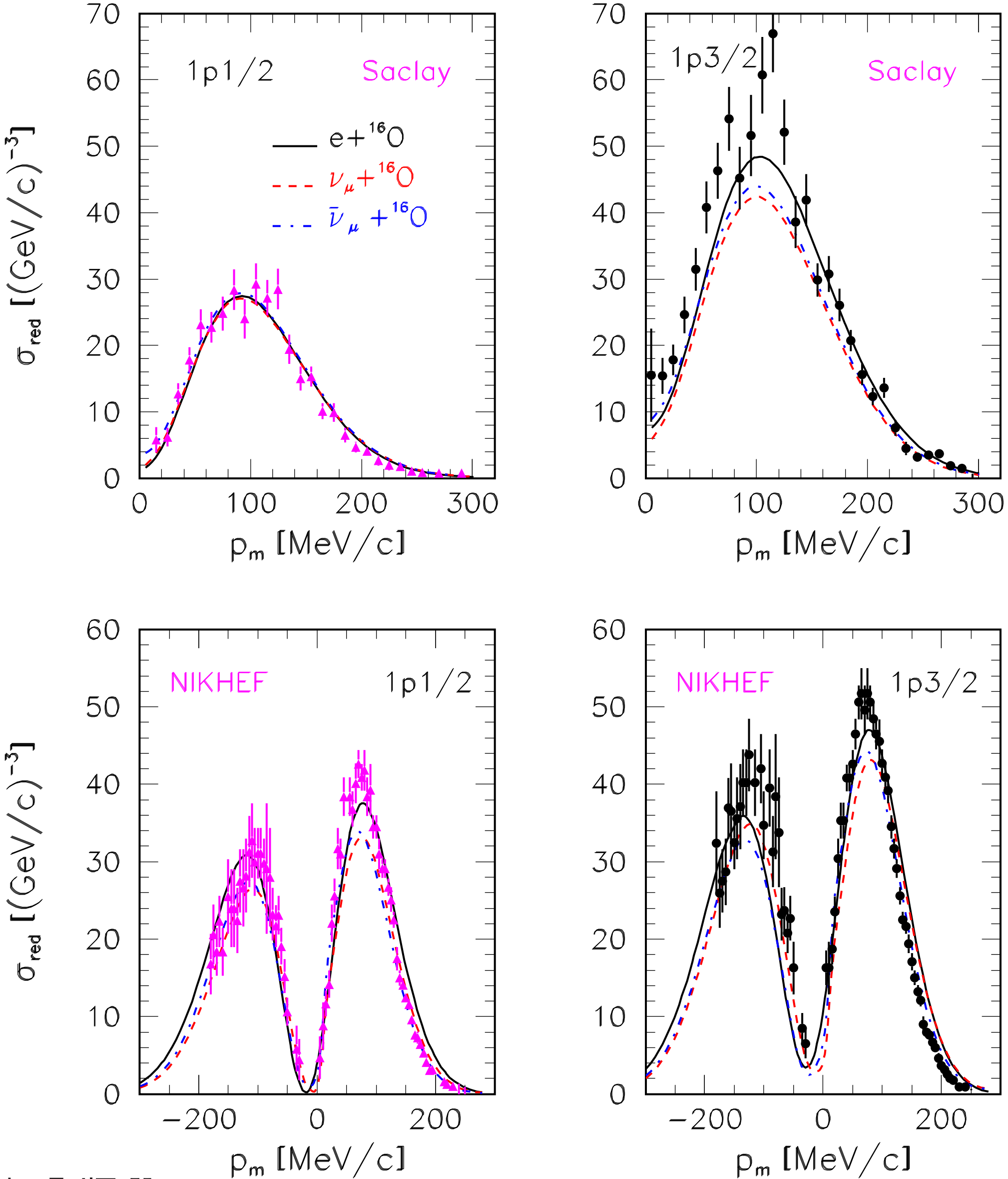

Comparison of the RDWIA electron, neutrino and antineutrino reduced cross sections for the removal of nucleons from 1p-shell of ^{16}O for Saclay (upper panels) and NIKHEF (lower panels) kinematic as functions of p_m. The solid line is electron while the dashed and dashed-dotted lines are respectively neutrino and antineutrino cross sections.

At the maximum electron cross section are higher (less than 10%) than (anti)neutrino ones.

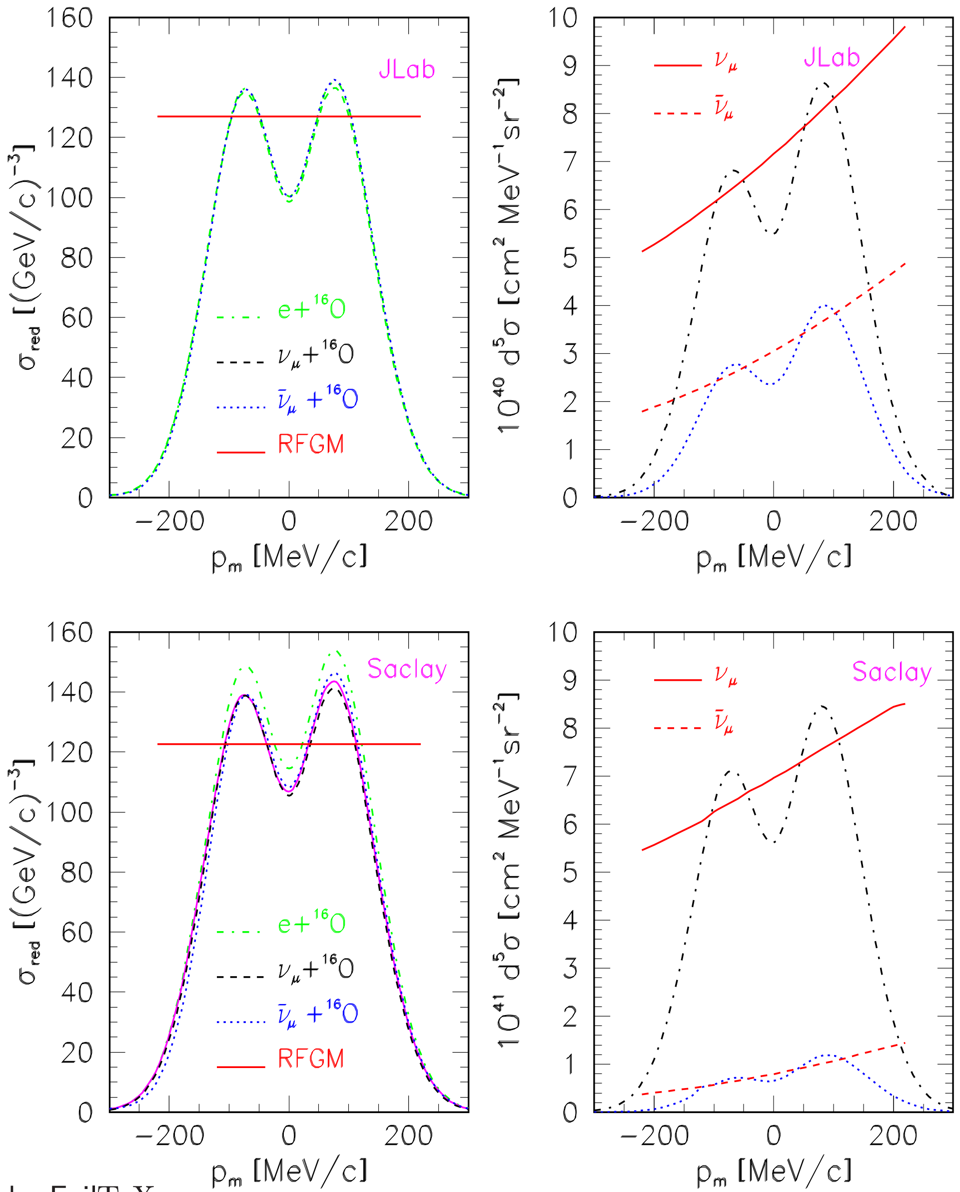

Comparison of the RDWIA and the RFGM calculations for electron, neutrino and antineutrino reduced and differential results for the removal of nucleons from 1p- and 1s-shells of ^{16}O. The dashed-dotted line is the RDWIA calculation for electron scattering while the dashed and dotted lines are respectively for neutrino and antineutrino scattering. The solid line on the left panels shows the RFGM result while the solid and dashed lines on the right panels are respectively neutrino and antineutrino cross sections calculated in the Fermi gas model. The dashed-dotted and dotted lines on right panels are respectively neutrino and antineutrino cross sections calculated in the RDWIA.

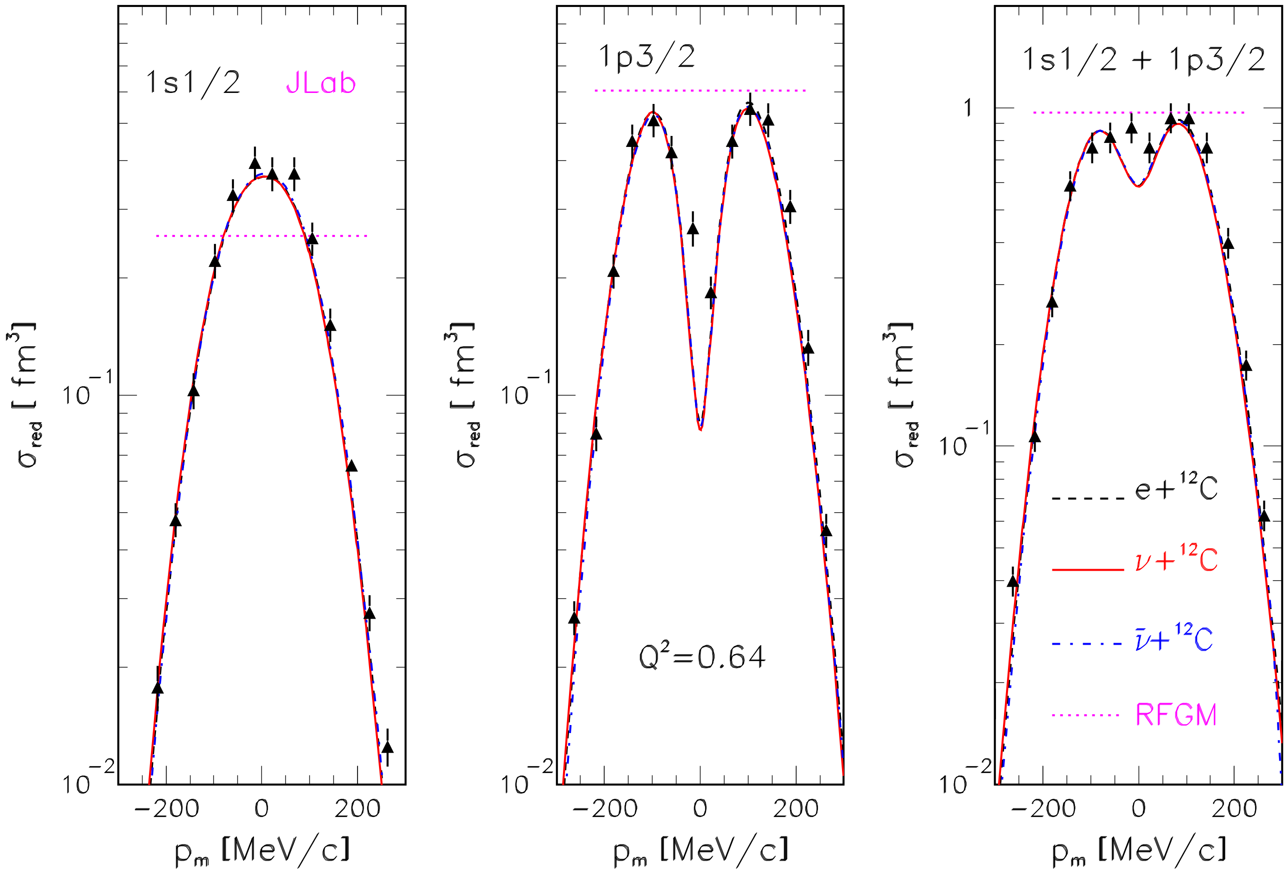

Comparison of the RDWIA and RFGM calculations for electron, neutrino, and antineutrino reduced cross sections for the removal of nucleon from $1p$ and $1s$ shells of ^{12}C as a function of missing momentum. The cross sections were calculated for JLab [D.Dutta et al. (2003)] kinematics: $\varepsilon_i = 2.445 GeV, Q^2 = 0.64 (GeV/c)^2$ and $T_x = 350 MeV$.
The RFGM predictions are completely off of the exclusive data (CCQE two-track events).

Analysis and Results

Low Q^2 problem

Charged-current QE events distributions as a function of Q^2 or $\cos\theta$ were measured by K2K and MiniBoone experiments. High statistic data show a disagreement with the RFGM prediction, $i.e.$ the data samples exhibit significant deficit in the region of low Q^2 ≤0.2 GeV^2 and small muon scattering angles.

Note that in the case of (anti)neutrino scattering off free nucleon CCQE differential cross sections $d\sigma^{\nu,\overline{\nu}}/dQ^2$ at $Q^2 \longrightarrow 0$ can be written as

$$\frac{d\sigma^{\nu,\overline{\nu}}}{dQ^2} = \frac{G^2}{2\pi}\cos^2\theta_c[F_V^2(0) + F_A^2(0)]$$

and do not depend on neutrino energy. The difference

$$\frac{d\sigma^{\nu}}{dQ^2} - \frac{d\sigma^{\overline{\nu}}}{dQ^2} = \frac{G^2}{\pi}\cos^2\theta_c\frac{Q^2}{m\varepsilon_i}\left(1 - \frac{Q^2}{4m\varepsilon_i}\right)(F_V + F_M)F_A$$

is proportional to F_A and decreases with neutrino energy. In the range of $\varepsilon_i \sim$ 0.5 ÷ 1 GeV it can be used for measuring of the axial form factor F_A.

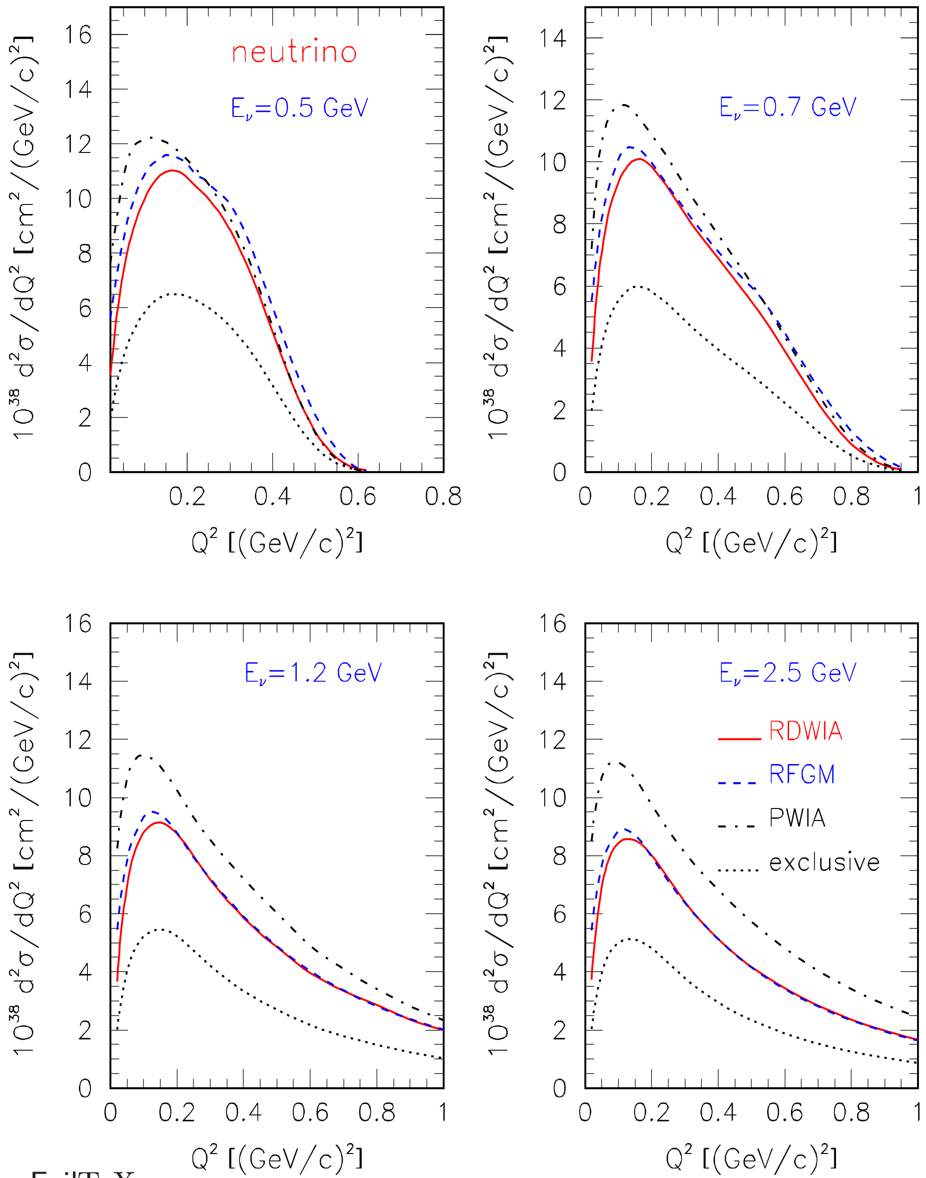

Inclusive cross section versus Q^2 for neutrino scattering on ^{12}C and for the four values of incoming neutrino energy: ε_ν=0.5, 0.7, 1.2 and 2.5 GeV. The solid line is the RDWIA calculation while the dashed and dashed-dotted lines are respectively the RFGM and PWIA calculations. The dotted line is the RDWIA result for the exclusive reaction (two-track events).

In the region < 0.2 (GeV/c)^2 the RFGM results are higher than those obtained in the RDWIA and at $Q^2 = 0.1$ (GeV/c)^2 the the difference is about $\sim 12\%$ for $\varepsilon_\nu = 0.5$ GeV and $\sim 6\%$ for $\varepsilon_\nu = 2.5$ GeV.

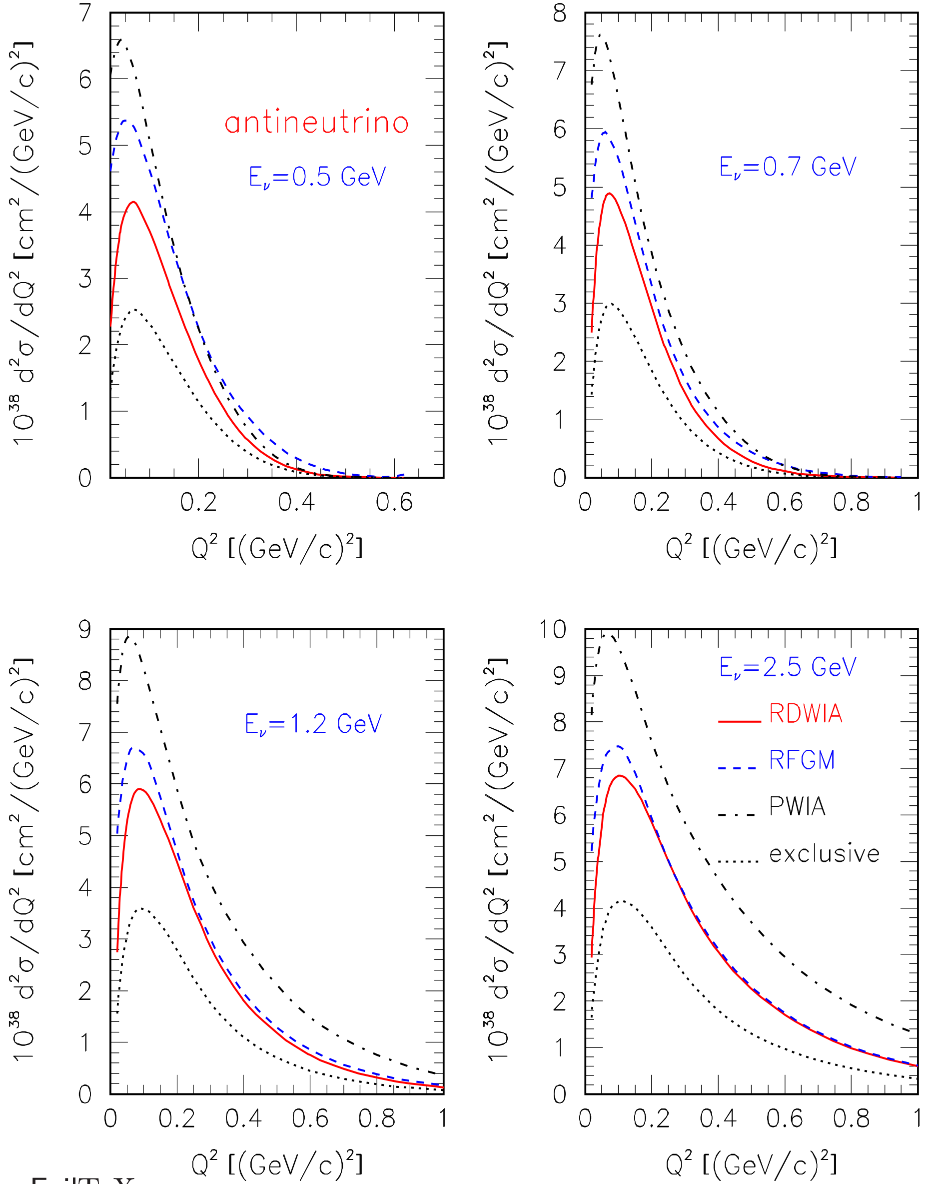

Inclusive cross section versus Q^2 for antineutrino scattering on ^{12}C and for the four values of incoming neutrino energy: ε_ν=0.5, 0.7, 1.2 and 2.5 GeV. The solid line is the RDWIA calculation while the dashed and dashed-dotted lines are respectively the RFGM and PWIA calculations. The dotted line is the RDWIA result for the exclusive reaction (two-track events).

In the region < 0.2 (GeV/c)^2 the RFGM results are higher than those obtained in the RDWIA and at $Q^2 = 0.1$ (GeV/c)^2 the the difference is about $\sim 29\%$ for $\varepsilon_\nu = 0.5$ GeV and $\sim 22\%$ for $\varepsilon_\nu = 2.5$ GeV.

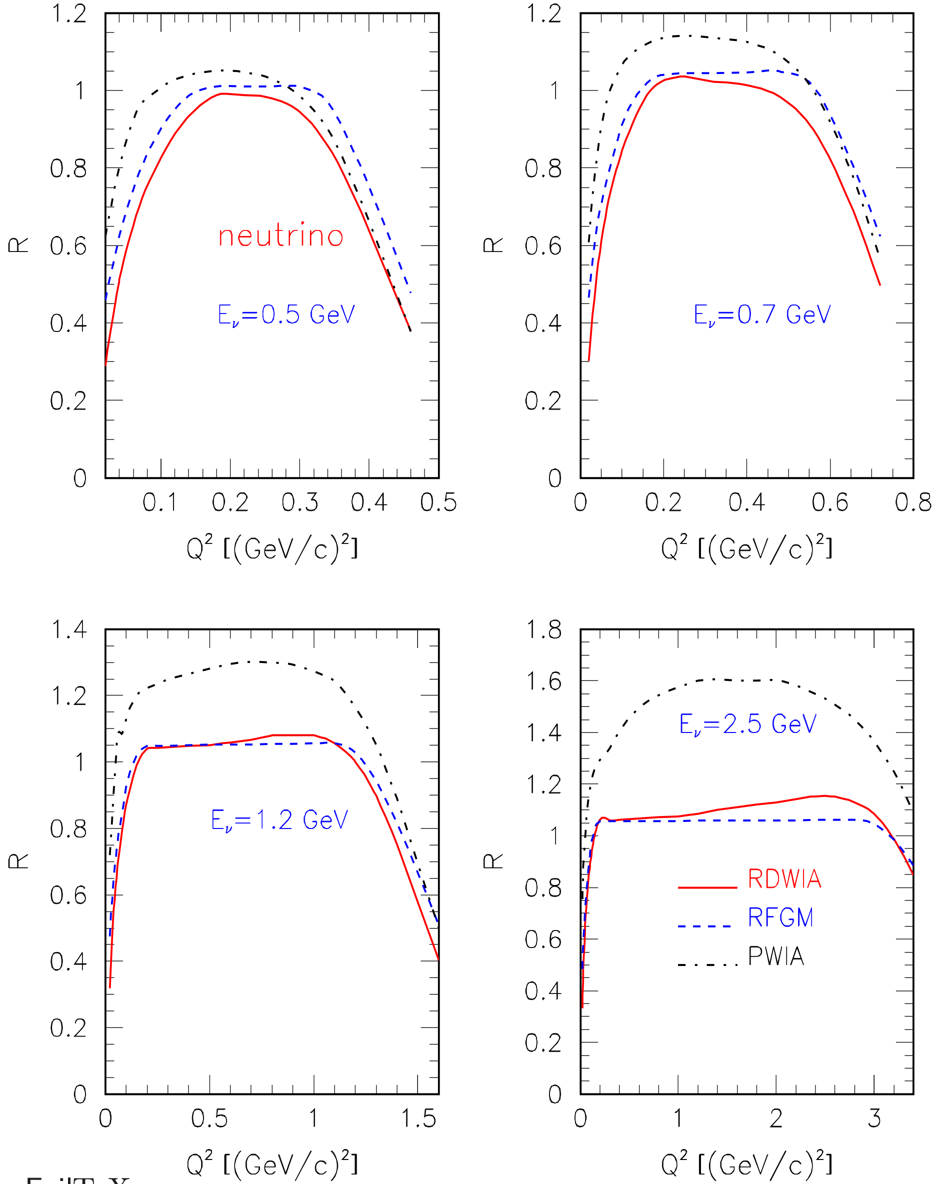

$R = (d\sigma/dQ^2)_{nuc}/(d\sigma/dQ^2)_{freenuc}$ versus Q^2 for neutrino scattering on ^{12}C and for the four values of incoming neutrino energy: ε_ν=0.5, 0.7, 1.2 and 2.5 GeV. The solid line is the RDWIA calculation while the dashed and dashed-dotted lines are respectively the RFGM and PWIA calculations.

Range of Q^2 where $R \approx const$, (i.e. nuclear effects cannot modify the value of M_A) increases with neutrino energy

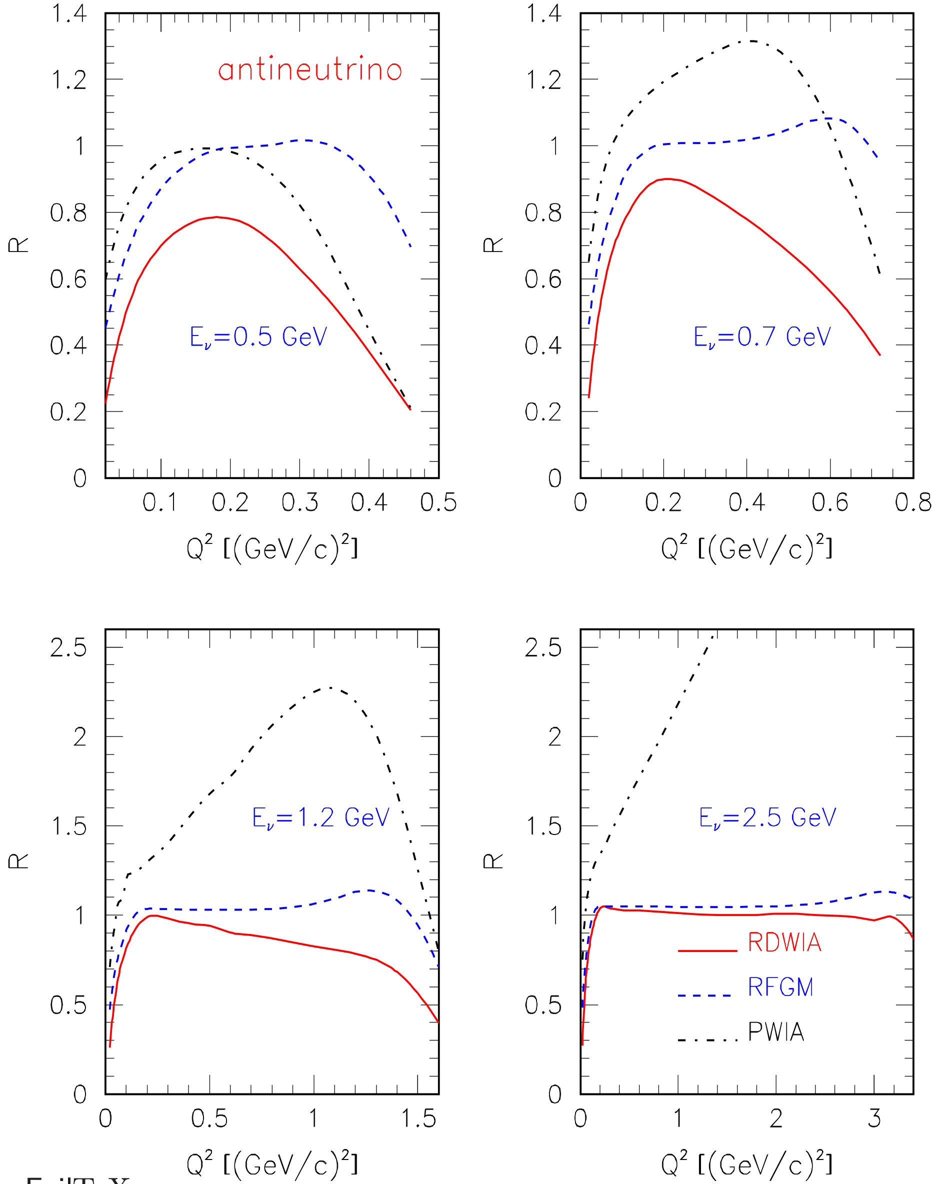

$R = (d\sigma/dQ^2)_{nuc}/(d\sigma/dQ^2)_{freenuc}$ versus Q^2 for antineutrino scattering on ^{12}C and for the four values of incoming neutrino energy: ε_ν=0.5, 0.7, 1.2 and 2.5 GeV. The solid line is the RDWIA calculation while the dashed and dashed-dotted lines are respectively the RFGM and PWIA calculations.

Selection of CCQE two-track events: nuclear-model dependence of the cut

- The two-track events are divided into two samples: QE and non QE enriched samples. Depending on detector capabilities dE/dx, information is applied to the second track for π/p separation.
- The measurement of the muon momentum and angle allows predict the angle of recoil proton assuming neutrino scattering off nucleon at rest.
- If the measured second track agrees with this prediction within $\Delta\theta$, it is likely a CCQE event.
- Using MC simulation based on the Fermi gas model the value of $\Delta\theta$ is chosen to give a reliable separation between the QE and non QE events.

We regard the angle θ_{pq} between the direction of outgoing proton and momentum transfer assuming that neutrino energy is reconstructed.

- For neutrino QE scattering on nucleon at rest $\boldsymbol{q} = \boldsymbol{p}_x$ and $\cos\theta_{pq}$ =1.
- For scattering off bound nucleon with momentum $\boldsymbol{p}_m$, $\boldsymbol{p}_x = \boldsymbol{p}_m + \boldsymbol{q}$ and

$$\cos\theta_{pq} = \frac{\boldsymbol{p}_x^2 + \boldsymbol{q}^2 - \boldsymbol{p}_m^2}{2|\boldsymbol{p}_x||\boldsymbol{q}|}.$$

- The maximal value of θ_{pq} corresponds to scattering on nucleon with maximal momentum $\boldsymbol{p}_{max}$, i.e.

$$\cos\theta_{pq}^{m} = \frac{\boldsymbol{p}_x^2 + \boldsymbol{q}^2 - \boldsymbol{p}_{max}^2}{2|\boldsymbol{p}_x||\boldsymbol{q}|}$$

and $\cos\theta_{pq}^{m} \leq \cos\theta_{pq} \leq 1$.

- In the RFGM, $\varepsilon_m = \sqrt{\boldsymbol{p}_m^2 + m^2} - \epsilon_b$, the recoil proton energy $\varepsilon_x = \sqrt{\boldsymbol{p}_m^2 + m^2} - \epsilon_b + \omega$ and for $|\boldsymbol{p}_{max}| = p_F$ we have

$$\boldsymbol{p}_x^2 = p_F^2 + \tilde{\omega}^2 + 2\tilde{\omega}\sqrt{p_F^2 + m^2},$$

where $\tilde{\omega} = \omega - \epsilon_b$.

- In the RDWIA the energy of an outgoing nucleon can be written as follow $\varepsilon_x = \omega + m_A - \varepsilon_B$ and we have

$$\cos\theta_{pq}^{m} = \frac{\bar{\omega}(2m + \bar{\omega}) + (Q^2 - m^2) - \boldsymbol{p}_{max}^2}{\sqrt{\bar{\omega}(2m + \bar{\omega})(Q^2 + m^2)}}, \tag{4}$$

where $\bar{\omega} = \omega - \langle\varepsilon_m\rangle - \boldsymbol{p}_{max}^2/2m_B^\star$, $m_B^\star = m_A - m + \langle\varepsilon_m\rangle$, $|\boldsymbol{p}_{max}|$=500 MeV/c, and mean missing energy for the shell nucleons $\langle\varepsilon_m\rangle = 27.1$ MeV.

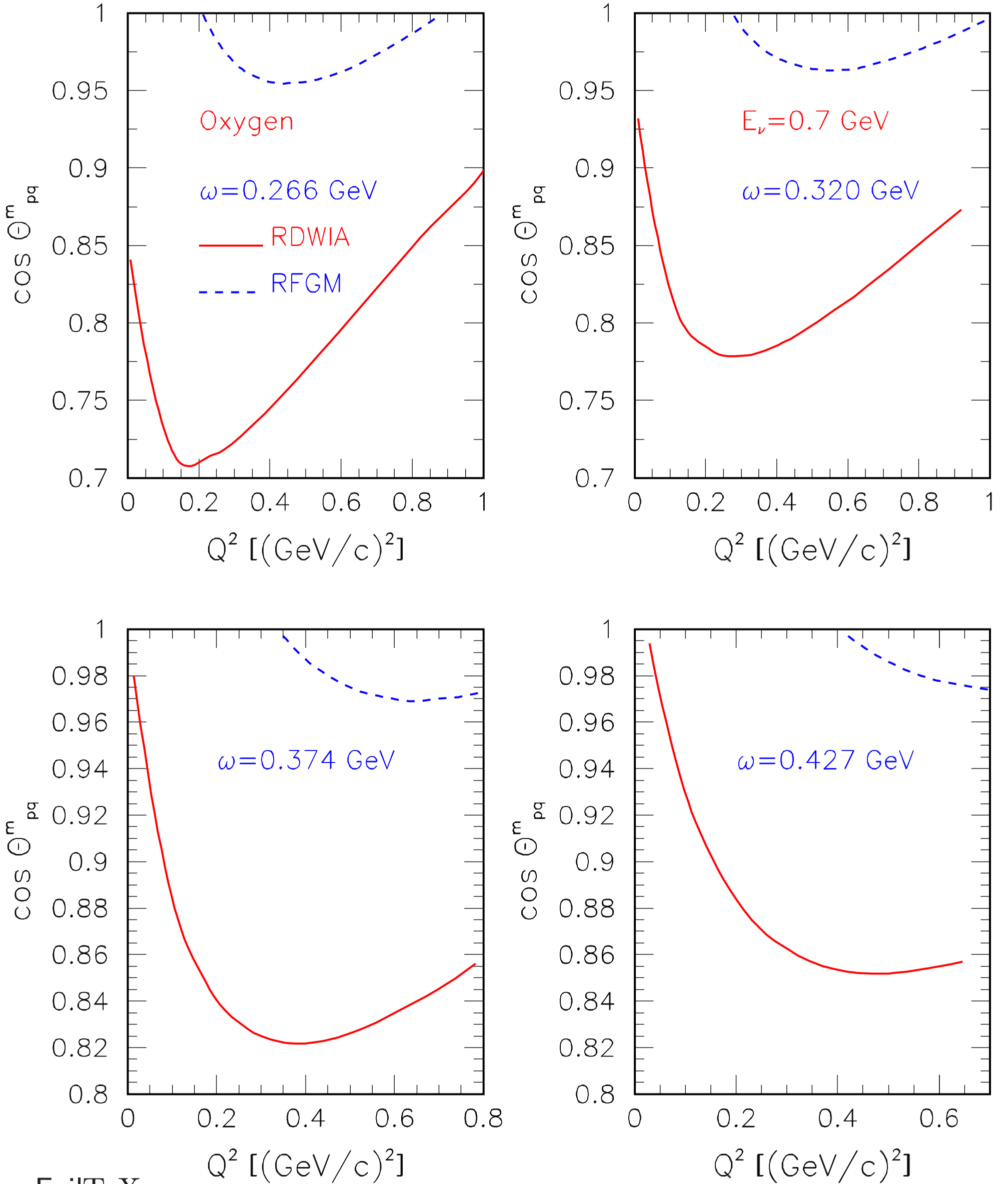

Contours of the phase volume in the $(\cos\theta_{pq}, Q^2)$ coordinates for neutrino scattering off ^{16}O with energy ε_ν=0.7 GeV and for the four values of energy transfer: ω=0.288, 0.320, 0.374 and 0.427 GeV. The solid line is the RDWIA calculation whereas the dashed line is the RFGM calculation.

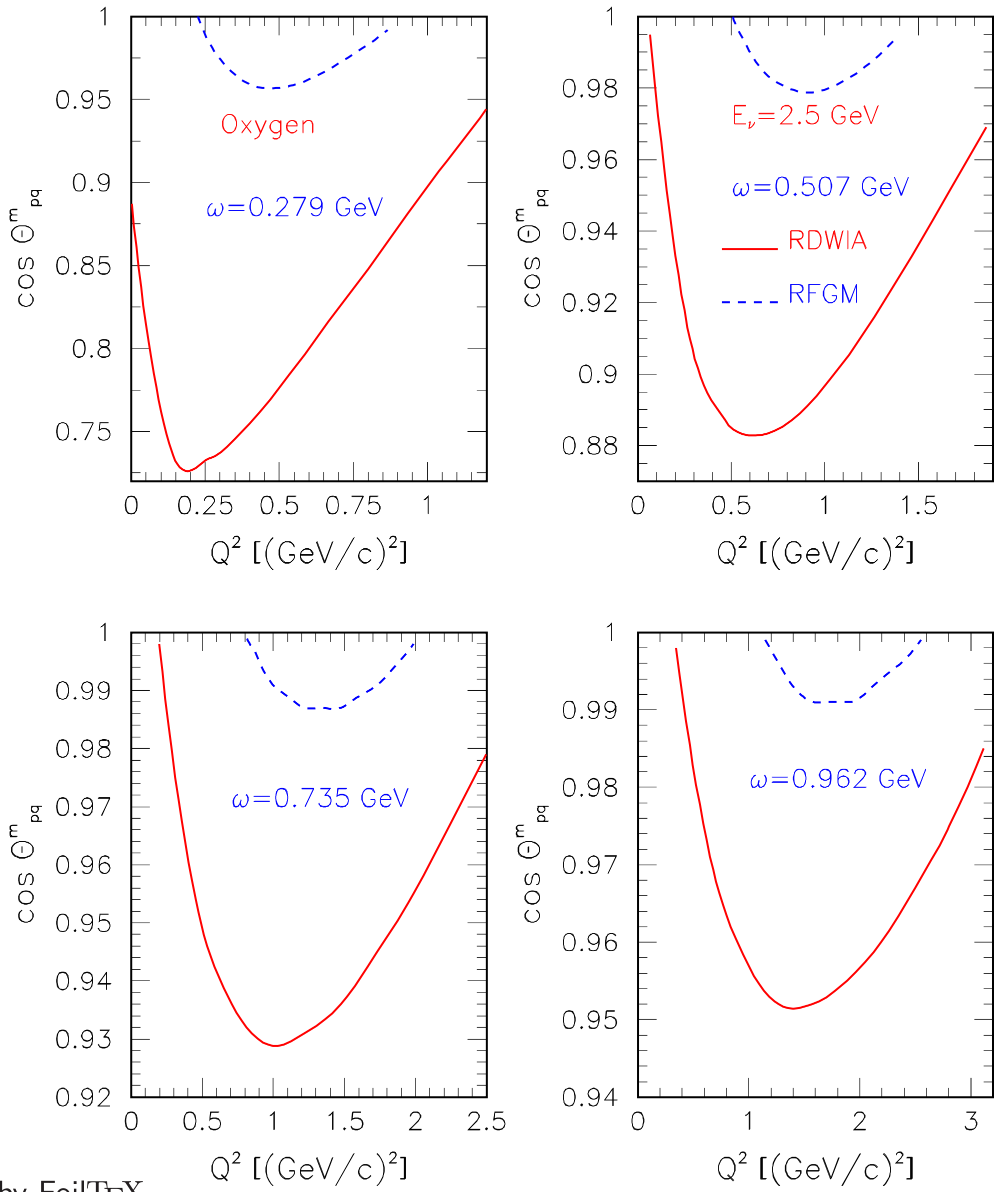

Contours of the phase volume in the $(\cos\theta_{pq}, Q^2)$ coordinates for neutrino scattering off ^{16}O with energy ε_ν=2.5 GeV and for the four values of energy transfer: ω=0.279, 0.507, 0.735 and 0.962 GeV. The solid line is the RDWIA calculation whereas the dashed line is the RFGM calculation. In the RDWIA kinematics the phase volume is larger then in the RFGM and the difference decreases with ω and neutrino energy.

Neutrino energy reconstruction

CCQE scattering

- Because the CCQE interaction represent a two-particle scattering process, it forms a good signal sample, and neutrino energy may be estimated using the kinematic of this reaction.
- There are two ways to measure the neutrino energy using CCQE events: kinematic or calorimetric reconstruction.

Kinematic reconstruction method

- In detectors with the energy threshold for proton detection $\varepsilon^p_{th} \geq 1$ GeV (Cherenkov detectors) the muon neutrino CCQE interactions will produce the one-track events. The kinematic reconstruction is applied for these events.
- Target nucleon is in rest

  The method is based on the assumption that the target nucleon to be at rest inside the nucleus and the correlation between the incident neutrino energy and a reconstructed muon momentum and scattering angle is used in this method.

$$\varepsilon_r = \frac{\varepsilon_f(m-\epsilon_b) - (\epsilon_b^2 - 2m\epsilon_b + m_\mu^2)/2}{(m-\epsilon_b) - \varepsilon_f + k_f\cos\theta}.$$

- Nucleon Fermi motion effect

  Using momentum $\boldsymbol{p}_x = \boldsymbol{p}_m + \boldsymbol{q}$ and energy balance the second order equation for neutrino energy which takes into account the bound nucleon momentum and energy distributions can be obtained.

$$A\varepsilon_r^2 - B\varepsilon_r + C = 0.$$

  Now the reconstructed energy ε_r is a function of $(\boldsymbol{p}_m, \varepsilon_m, \cos\tau)$, where $\cos\tau = \boldsymbol{p}_m \cdot \boldsymbol{q}/|\boldsymbol{p}_m \cdot \boldsymbol{q}|$

- Moments of the reconstructed neutrino energy

  The distribution $\varepsilon_r(\boldsymbol{p}_m, \varepsilon_m, \cos\tau)$ corresponds to measured values of $(k_f, \cos\theta)$ and at $\varepsilon_m, \boldsymbol{p}_m \to 0$ has an asymptotic form given by the formula for nucleon at rest.
  The n-th moment of $\varepsilon_r(k_f, \cos\theta, \boldsymbol{p}_m, \varepsilon_m)$ distribution versus of k_f and $\cos\theta$ can be written as

$$\langle\varepsilon_r^n(k_f, \cos\theta)\rangle = \int_{p_{min}}^{p_{max}} d\boldsymbol{p} \int_{\varepsilon_{min}}^{\varepsilon_{max}} S(\boldsymbol{p}, \varepsilon)[\varepsilon_r(k_f, \cos\theta, \boldsymbol{p}, \varepsilon)]^n d\varepsilon,$$

  where $S(\boldsymbol{p}, \varepsilon)$ is the probability density function (pdf) for the target nucleon momentum and energy distribution being normalized with respect to the unit area.

- The mean of $\varepsilon_r(k_f, \cos\theta)$ and its variance $\sigma^2(\varepsilon_r)$ are defined by
  $\bar{\varepsilon}_r(k_f, \cos\theta) = \langle\varepsilon_r(k_f, \cos\theta)\rangle, \sigma^2(\varepsilon_r) = \langle\varepsilon_r^2(k_f, \cos\theta)\rangle - \bar{\varepsilon}_r^2(k_f, \cos\theta)$

Accuracy of reconstructed neutrino energy

- The accuracy of reconstructed energy $\varepsilon_r(\varepsilon_i)$ as a function of ε_i can be estimated using the moments of $\varepsilon_r(k_f, \cos\theta)$ distribution

$$\langle\varepsilon_r^n(\varepsilon_i)\rangle = \int dk_f \int W(k_f, \cos\theta)[\varepsilon_r(k_f, \cos\theta)]^n d\cos\theta,$$

  where $W(k_f, \cos\theta)$ is the pdf of the muon momentum and scattering angle.

- $[\varepsilon_r(k_f, \cos\theta)]^n = \langle\varepsilon^n(k_f, \cos\theta)\rangle$ if the nucleon Fermi motion effect is taken into account, or $\varepsilon_r(k_f, \cos\theta)$ is given by formula for nucleon which is at rest, if this effect is neglected.

- The reconstructed neutrino energy $\bar{\varepsilon}_r = \langle\varepsilon_r\rangle$ is smeared with variance $\sigma^2(\varepsilon_i) = \langle\varepsilon_r^2(\varepsilon_i)\rangle - \bar{\varepsilon}_r^2(\varepsilon_i)$ and biased with $\Delta(\varepsilon_i) = \varepsilon_i - \bar{\varepsilon}_r$

- The detailed description of this approach is given in [A.Butkevich PRC78:015501,(2008)].

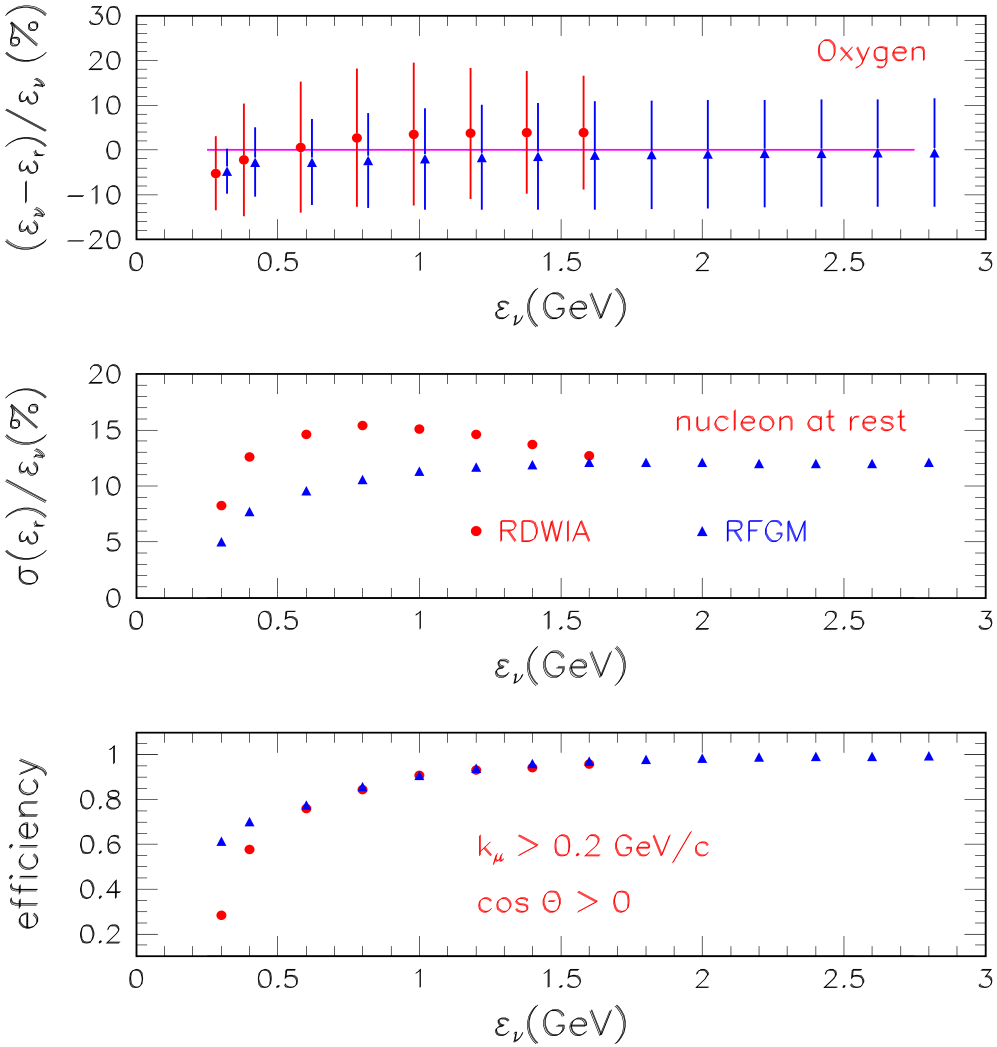

Bias (top panel), variance (middle panel) of the reconstructed neutrino energy, and efficiency (bottom panel) of the one-track events detection with $k_f \geq$0.2 (GeV/c) and $\cos\theta \geq$0 as functions of neutrino energy. The Neutrino energy reconstruction was formed assuming the target nucleon is at rest inside nucleus. The vertical bars show $\sigma[(\varepsilon_i - \varepsilon_r)/\varepsilon_i]$. As displayed in the key, biases, variances, and efficiencies were calculated in the RDWIA and RFGM.

RFGM: in range $0.3 \div 2.5$ $\Delta = -4.7\% \rightarrow \Delta = -0.7\%$ and $\sigma/\varepsilon_i = 5.4\% \rightarrow \sigma/\varepsilon_i = 12\%$.

RDWIA: in range $0.3 \div 1.6$ $\Delta = -5.2\% \rightarrow \Delta = 3.9\%$ and $\sigma/\varepsilon_i = 8.3\% \rightarrow \sigma/\varepsilon_i = 12.7\%$.

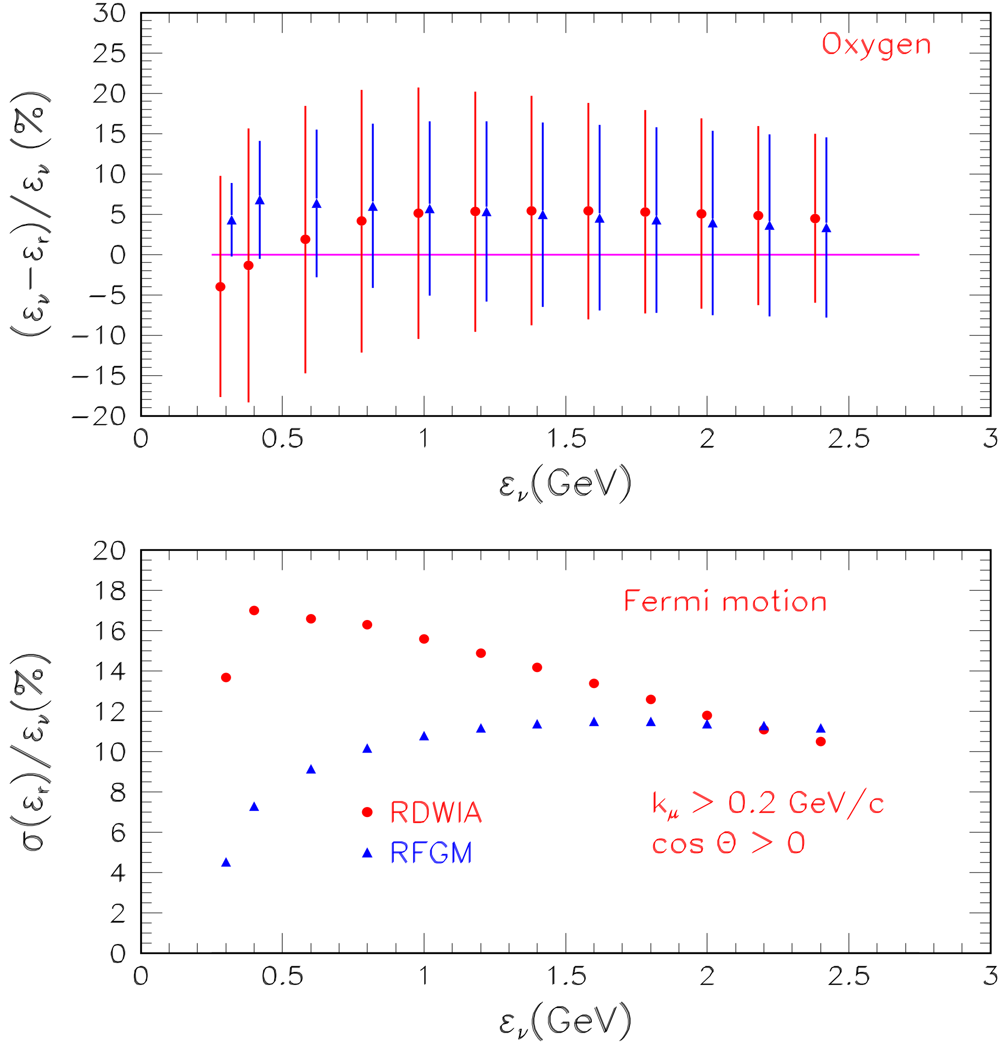

Bias (top panel) and variance (bottom panel) of the reconstructed neutrino energy as functions of neutrino energy. The energy reconstruction was formed taking into account the nucleon momentum distribution in the target with $E_{max} = 10$ GeV. As displayed in the key, biases and variances were calculated in the RDWIA and RFGM.

RFGM: in range $0.3 \div 2.5$ $\Delta = 4.3\% \rightarrow \Delta = 3\%$ and $\sigma/\varepsilon_i = 4.6\% \rightarrow \sigma/\varepsilon_i = 11\%$.

RDWIA: in range $0.3 \div 2.5$ $\Delta = -4\% \rightarrow \Delta = 4.5\%$ and $\sigma/\varepsilon_i = 14.3\% \rightarrow \sigma/\varepsilon_i = 10.5\%$.

Note: Bias may depend on the value of E_{max}.

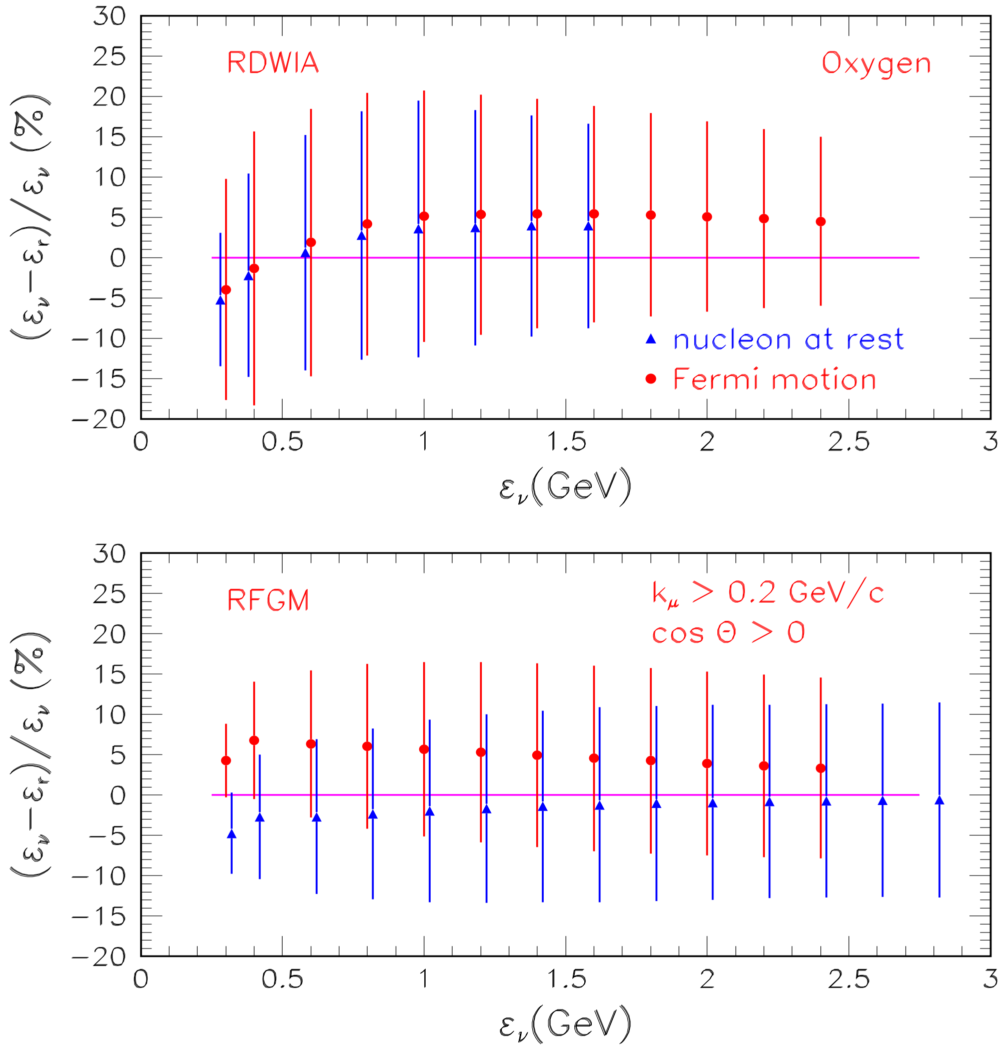

Biases calculated in the RDWIA (top panel) and RFGM (bottom panel) as functions of neutrino energy. As displayed in the key, energy reconstructions were formed with and without the nucleon momentum distribution. The biases calculated within the RDWIA and RFGM assuming that nucleon is at rest (Δ_{fr}) and using the mean energy method (Δ_{me}) are presented as functions of neutrino energy. In the RDWIA approach the nucleon Fermi motion effect leads to increase the bias by about 1.2%. In the Fermi gas model with this effect ε_r is overestimated and $\Delta_{fr}(\Delta_{me}) = -4.7\%(4.3\%)$ for energy 0.3 GeV and $\Delta_{fr}(\Delta_{me}) = -0.7\%(3.4\%)$ for $\varepsilon_\nu = 2.5$ GeV.

- Apparently the accuracy of the kinematical reconstruction neutrino energy for one-track events depends on the nuclear models of QE neutrino CC interaction with nuclei and on the neutrino energy reconstruction methods.

- We can estimate the systematic uncertainties of this approach by comparing Δ_{FG} and δ_{FG} calculated in the RFGM with Δ_R and δ_R evaluated in the RWDIA approach using the mean energy method.

- It is clear that uncertainties depend on neutrino energy and the bias uncertainty increases with energy from $(\Delta_R - \Delta_{FG}) \approx 0.7\%$ for $\varepsilon_\nu = 0.3$ GeV up to 5.2% for $\varepsilon_\nu = 2.5$ GeV and the energy resolution uncertainty decreases with increasing energy from $\delta_R - \delta_{FG} \approx 8.3\%$ to 0.5% in this energy range.

For the two-track events the moments of the $\varepsilon_r(k_f, \cos\theta)$ distribution can be written as

$$\langle \varepsilon_r^n(\varepsilon_i)\rangle = \sum_\alpha w_\alpha \langle \varepsilon_r^n(\varepsilon_i)\rangle_\alpha,$$

where

$$\langle \varepsilon_r^n(\varepsilon_i)\rangle_\alpha = \int dk_f \int d\cos\theta \int_0^{2\pi} d\phi \int_{p_{min}}^{p_{max}} [\varepsilon_f + T_p + \langle \varepsilon_m \rangle]^n W_\alpha(k_f, \cos\theta, \phi, p_m) dp_m,$$

$$W_\alpha = \frac{1}{\sigma_\alpha^{ex}} \Big[\frac{d^5\sigma}{dk_f d\cos\theta d\phi dp_m}\Big]_\alpha$$

$$\sigma_\alpha^{ex} = \int dk_f \int d\cos\theta \int_0^{2\pi} d\phi \int_{p_{min}}^{p_{max}} \Big[\frac{d^5\sigma}{dk_f d\cos\theta d\phi dp_m}\Big]_\alpha dp_m,$$

$$w_\alpha = \sigma_\alpha^{ex} / \sum_\alpha \sigma_\alpha^{ex}$$

and $d^5\sigma/dk_f d\cos\theta d\phi dp_m$ is the QE neutrino CC scattering exclusive cross section.

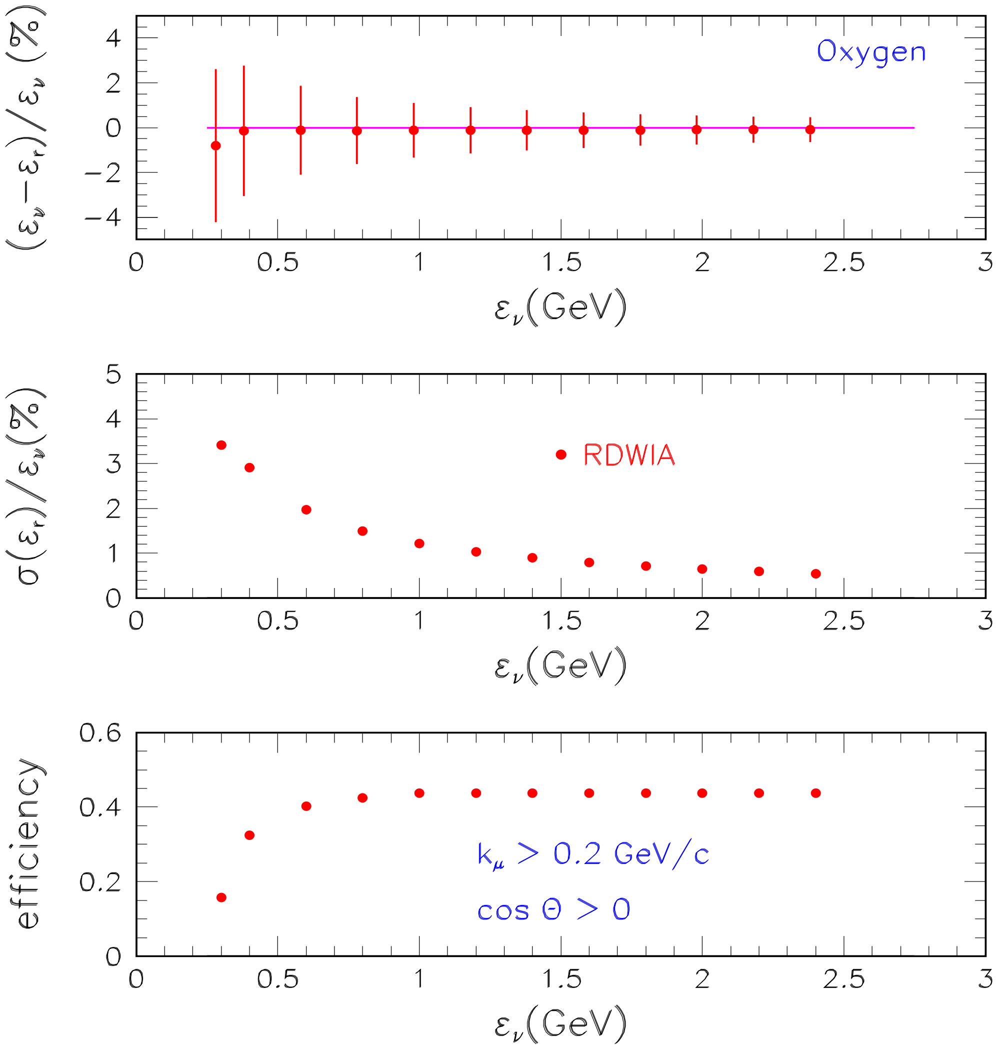

In the calorimetric reconstruction ε_r is formed as the sum of muon energy ε_f, kinematic proton energy T_p and mean missing energy $\langle\varepsilon_m\rangle$
$\varepsilon = \varepsilon_f + T_p + \langle\varepsilon_m\rangle$.
Bias (top panel), variance (middle panel) of the reconstructed neutrino energy, and efficiency (bottom panel) of the two-tracks events detection with $k_f \geq$0.2 (GeV/c) and $\cos\theta \geq$0 and without any cuts for proton. At $\varepsilon_\nu > 0.3$ (GeV) $\Delta = -0.1\%$. The energy resolution: 3.4% at $\varepsilon_\nu = 0.3$ (GeV) and 0.5% at $\varepsilon_\nu = 2.5$ (GeV). The challenge is identifying proton track and reconstructing its kinetic energy with reliable accuracy at low threshold energy for proton detection.

Summary

QE CC $\nu(\bar{\nu})^{16}$O and ^{12}C cross sections were studied in different approaches.

- The reduced cross sections for neutrino and electron scattering off ^{12}C were tested against ^{16}O and ^{12}C(e,e'p) data. The RFGM fails completely when compared to exclusive cross section data.
- At $Q^2 > 0.2$ (GeV/c)^2 the nuclear effects slight change the slope in the Q^2 distribution. The size of this range ΔQ^2 increases with neutrino energy and practically does not depend on the nuclear models. This range is preferable for the M_A analysis to reduce the uncertainty from the nuclear model.
- We showed that the efficiency and purity of the CCQE two-track events selection are nuclear model dependent and the difference decreases with increasing energy transfer and neutrino energy.
- We studied the nuclear-model dependence of the energy reconstruction accuracy, neglecting by systematics related to event selection and resolution. We found that the accuracy of the kinematic reconstruction for one-track events depends on the nuclear model of CCQE neutrino interaction and neutrino energy reconstruction method.
- In the case of two-track events accuracy may be higher and does not depend on nuclear models of CCQE neutrino-nucleus interaction.